Paper:

Strength and Deformation of Confined Brick Masonry Walls Subjected to Lateral Forces – Review of Existing Test Data in Japan and Peru –

Shunsuke Sugano*, Taiki Saito, Carlos Zavala***, and Lourdes Cardenas*****

*Building Research Institute
1 Tachihara, Tsukuba, Ibaraki 305-0802, Japan
E-mail: sugano@hiroshima-u.ac.jp
**Toyohashi Institute of Technology, Toyohashi, Japan
***Centro Peruano Japonés de Investigaciones Sísmicas y Mitigación de Desastres (CISMID), Lima, Peru
[Received August 11, 2014; accepted November 5, 2014]

The Japanese and Peruvian experimental databases on confined brick masonry walls are put together as one database, and the strength and deformation of the walls are reviewed. First, the applicability of existing equations for the ultimate strength of reinforced concrete or reinforced masonry walls to the estimation of the maximum strength of confined brick masonry walls which failed in shear, flexural-shear, or flexure when subjected to lateral forces, is discussed. Then, empirical equations for the maximum strength, displacement at maximum strength, and ultimate state of the walls are proposed based on multiple regression analysis, and the accuracy of the proposed equations is discussed. It is concluded that the maximum strength can be estimated using the existing equations or the proposed empirical equations with good accuracy. The deformations at maximum strength and the ultimate state can be estimated using the proposed empirical equations, although there is a large amount of scatter.

Keywords: confined masonry, test data, strength, deformation, lateral force, backbone model

1. Introduction

The Building Research Institute (BRI) of Japan has been collecting research papers and test data on reinforced masonry (RM) and confined masonry (CM) walls from all over the world to propose a backbone model for the design and analysis of masonry buildings subjected to lateral forces. The Centro Peruano-Japonés de Investigaciones Sísmicas y Mitigación de Desastres (CISMID) of Peru has also been collecting papers and test data on confined brick masonry walls in Latin American countries for the same purpose.

In this paper, the Japanese [1–3] and Peruvian databases [4–6] on confined brick masonry walls (**Figs. 1** and **2**) are put together and reviewed with respect to the failure mode, the maximum strength, the deformations at maximum strength, and the ultimate state of walls subjected to lateral forces.

This paper describes (1) the applicability of existing equations for the design and analysis of reinforced concrete walls or reinforced masonry walls to the experimental maximum strengths of confined brick masonry walls, (2) the factors that affect the strength and deformability of confined brick masonry walls, (3) multiple regression analyses of the maximum strength, the deformations at maximum strength, and the ultimate states of walls.

2. Outline of Experimental Database

2.1. Japanese Database

Since 1992, the Chiba Institute of Technology, Building Research Institute, Oita University, Akita University, the University of Tokyo, Hokkaido University, and Mie University have conducted tests on confined masonry walls under static cyclic loading. Among them, the test data of Building Research Institute [1] and Oita University [2, 3] were selected as the database for the review in this study because (1) a large number of test specimens were included in a series of tests and (2) the effects of many structural factors on the behavior of confined brick masonry walls were studied.

There are 55 walls in total in the Japanese database, and the ranges of structural factors are as follows: prism compressive strength of brick masonry, F_m: 18.5–60.6 N/mm^2; wall length l: 1,070–1,750 mm; wall thickness t: 100–183 mm; wall height h: 665–1,663 mm; shear span ratio, h/l: 0.52–0.95; column reinforcement ratio, P_{te}: 0.05–0.67%; wall lateral reinforcement ratio, P_{we}:0.00–0.64%; and axial stress, σ_0: 0.39–1.37 N/mm^2.

2.2. Peruvian Database

The Peruvian database consists of the experimental data on the 34 confined brick masonry walls tested in the CISMID since 1993 [4–6]. The ranges of structural factors are as follows: prism compressive strength of

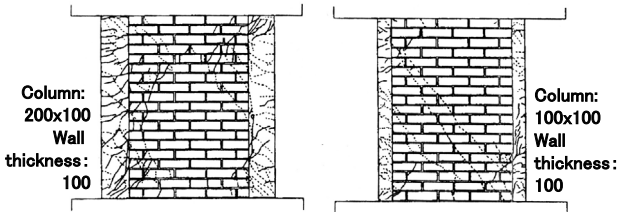

Fig. 1. Confined brick masonry walls in the test of Building Research Institute in 1994 [1].

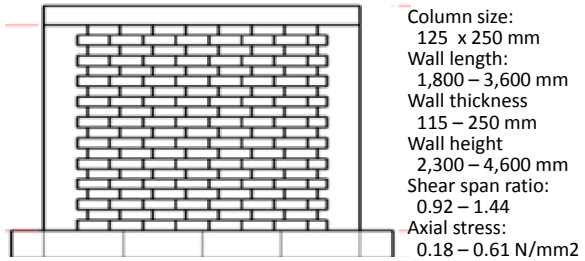

Fig. 2. Confined brick masonry walls in the test of CISMID in peru [4–6].

masonry, F_m: 2.2–29.8 N/mm^2; wall length, l: 1,800–3,600 mm; wall thickness, t: 120–250 mm; wall height, h: 2,300–3,450 mm; wall shear span ratio, h/l: 0.64–1.44; column reinforcement ratio, P_{te}: 0.05–0.20%; wall lateral reinforcement ratio, P_{we}: 0.23–0.28%; and axial stress, σ_0: 0.18–0.61 N/mm^2.

3. Load – Deformation Relationship

In the review of the database, the envelope of hysteresis curves of each wall tested was idealized into the four-line backbone curve shown in **Fig. 3**. The curve has three breaking points where stiffness changes: the cracking point (C), yielding point (Y), and maximum strength point (Max), and ultimate point (Ult). The ultimate point is defined as the point where the strength decreases to 80% of the maximum strength. The yielding point is defined as the point where the observed strain at the flexural reinforcement exceeds the yield strain or as the point where significant change in stiffness is observed in the hysteresis curves.

The failure mode of a wall which has failed in shear without yielding is defined as "shear failure" and is abbreviated as "S" in this paper. The failure mode of a wall which has failed in shear after yielding is defined as "flexural-shear failure" and is abbreviated as "FS." The failure mode of a wall which has failed in flexure is defined as "flexural failure" and is abbreviated as "F."

4. Application of Existing Equations

The applicability of existing equations for the design and analysis of reinforced concrete walls or reinforced

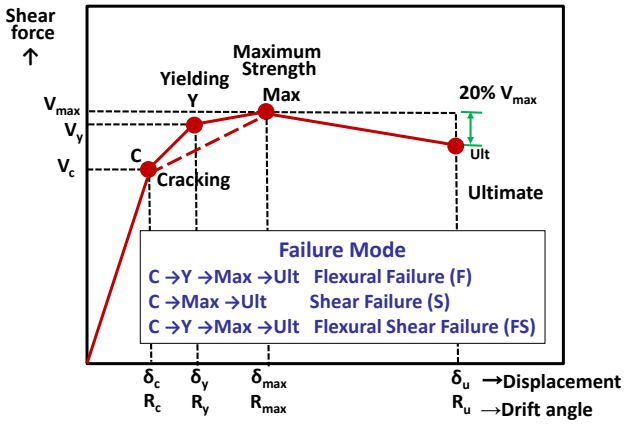

Fig. 3. Backbone model of restoring force characteristics of confined brick masonry walls.

masonry walls to confined brick masonry walls is determined by comparing the observed maximum strength to the strength calculated using the equations.

4.1. Existing Equation for Ultimate Shear Strength of Reinforced Concrete Shear Walls

For design and analysis of reinforced concrete shear walls, the following equation is used to calculate the lower boundary of the observed shear strength in tests.

$$Q_{su1} = \left\{ \frac{0.053 \cdot p_{te}^{0.23}(F_m + 18)}{M/(Q \cdot l) + 0.12} + 0.85\sqrt{p_{we} \cdot \sigma_{wy}} + 0.1\overline{\sigma_{0e}} \right\} \cdot t_e \cdot j \quad \cdots \quad (1)$$

where t_e: wall thickness and $t_e = A_w/l$, A_w: section area of wall, l: wall length, P_{te}: tensile reinforcement ratio ($= 100a_t/(t_e l_w)$, unit %), a_t: section area of tensile reinforcement (mm^2), F_m: compressive strength of masonry prism (N/mm^2), l_w: wall effective length $= 0.9l$, P_{we}: lateral reinforcement ratio ($= a_w/t_e s$) (must be 0.012 when it exceeds 0.012), a_w: section area of a pair of lateral reinforcements and s: its space, σ_{wy}: yield strength of lateral reinforcement (N/mm^2), j: distance between centers of tensile and compressive stresses ($= (7/8)l_w$), σ_{0e}: average axial stress of wall (N/mm^2) ($= N_w/A_w$), N_w: axial force acting on the wall (N), $M/(Ql)$: shear span ratio $= h/l$, h: height of inflection (loading) point, which must be 1.0 when it is less than or equal to 1.0 and 3.0 when it exceeds 3.0.

Figure 4 shows the relationship between observed strength and the strength calculated by Eq. (1), both in terms of the average shear stress in N/mm^2. Eq. (1) overestimates the maximum strength for most shear failure walls and overestimates more for all the flexural-shear failure or flexural failure walls.

4.2. Equation for Shear Strength of Masonry Walls

The following equation has been proposed by the Architectural Institute of Japan as the equation to use to evaluate the ultimate shear strength of reinforced masonry walls subjected to lateral forces [8]. The equation is

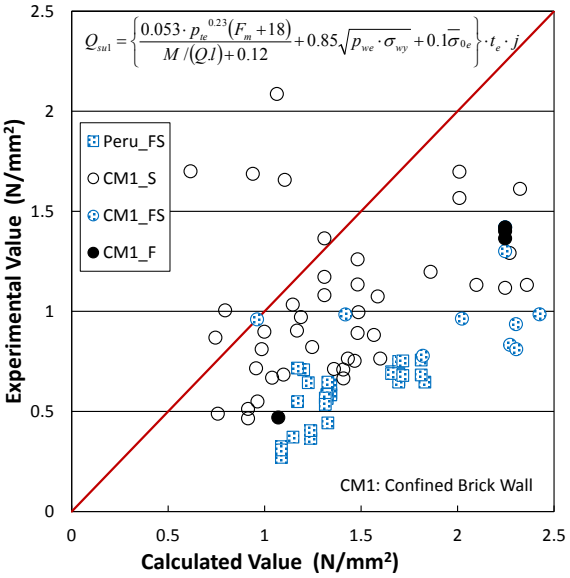

Fig. 4. Evaluation of the maximum strength using existing equation for shear strength of RC walls.

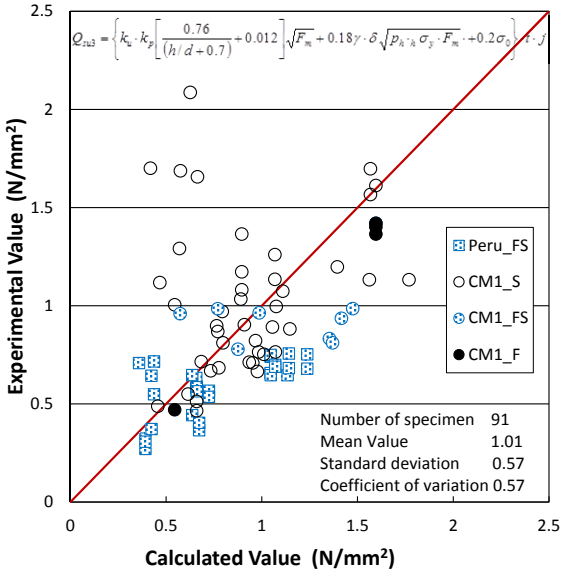

Fig. 5. Evaluation of the maximum strength using AIJ equation for shear strength of hollow concrete block walls.

based on tests conducted by Matsumura on hollow concrete block walls [9].

$$Q_{su3} = \left\{ k_u \cdot k_p \left[\frac{0.76}{h/d+0.7} + 0.012 \right] \sqrt{F_m} + 0.18\gamma \cdot \delta \sqrt{p_h \cdot {}_h\sigma_y \cdot F_m} + 0.2\sigma_0 \right\} \cdot t \cdot j \quad (2)$$

where k_u: reduction factor depending on masonry material ($k_u = 0.64$ [8]), k_p: $1.16 p_t^{0.3}$ ($p_t = 100 a_t/(t \cdot d)$, unit %), h: height of inflection point$\times 2$, d: effective length of wall ($= l_0 - t/2$), l_0: wall length, t: wall thickness, a_t: section area of tensile reinforcements (mm^2), F_m: compressive strength of masonry prism (N/mm^2), γ: reduction factor depending on reinforcement ($\gamma = 0.6$ [8]), δ: reduction factor depending on loading condition ($\delta = 1.0$ [8]), p_h: lateral reinforcement ratio ($= a_w/ts$), a_w: section area of a pair of lateral reinforcements and s: space of the pair of lateral reinforcements, ${}_h\sigma_y$: yield strength of lateral reinforcement (N/mm^2), σ_0: average axial stress of wall (N/mm^2), N_w: axial force acting on the wall (N), and j: distance between centers of tensile and compressive stresses ($= (7/8)d$).

Figure 5 shows the relationship between observed maximum strength in test and the calculated shear strength using Eq. (2), where the strengths are expressed in terms of the average shear stress in N/mm^2. It has been observed that Eq. (2) provides the average of the observed maximum strength, though there is a significant amount of scatter. It is interesting that Eq. (2) provides the average of the test results of confined brick masonry walls despite the fact that it is based on the test results from hollow concrete block walls, another type of wall altogether.

4.3. Approximate Equation for Flexural Strength

The following equation is used to approximate the ultimate flexural strength of reinforced concrete walls. It is known that this equation predicts the ultimate flexural strength of walls well even though it is an approximate equation based on simple assumptions.

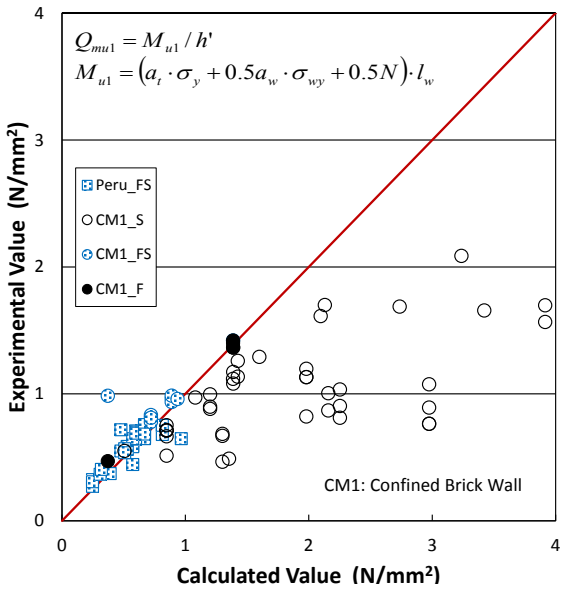

Fig. 6. Evaluation of the maximum strength using the approximate equation for ultimate flexural strength.

$$\begin{aligned} Q_{mu1} &= M_{u1}/h' \\ M_{u1} &= (a_t \cdot \sigma_y + 0.5 a_w \cdot \sigma_{wy} + 0.5N) \cdot l_w \quad . \end{aligned} \quad (3)$$

where M_{u1}: flexural strength of wall, h': height of the inflection (loading) point, a_t: section area of tensile reinforcement (mm^2), σ_y: yield strength of tensile reinforcement (N/mm^2), a_w: section area of vertical reinforcements in the wall section (mm^2), σ_{wy}: yield strength of vertical reinforcements in the wall section (N/mm^2), l: length of wall, l_w: wall length $\times 0.9$, and N: axial force (N).

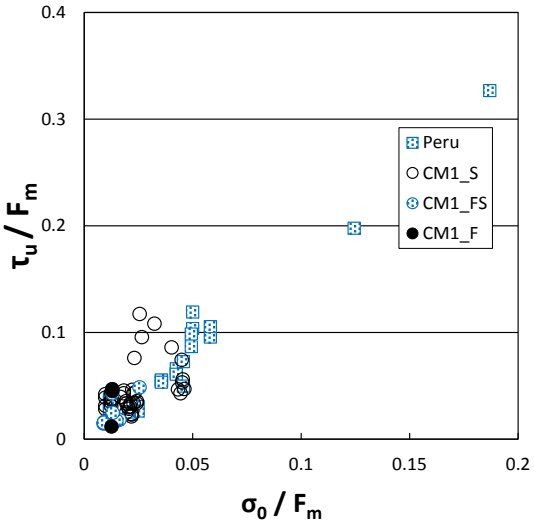

Fig. 7. Maximum strength vs axial stress ratio.

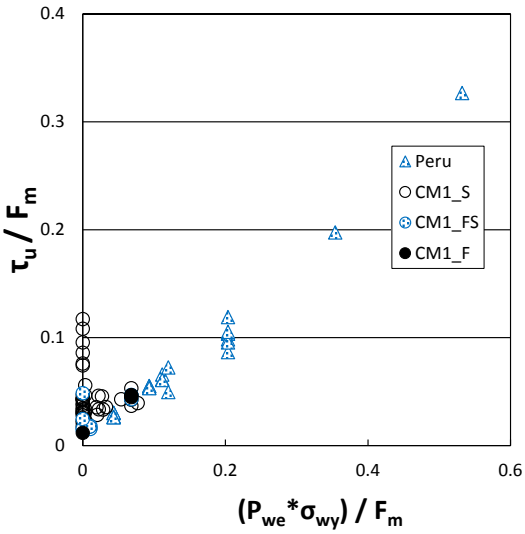

Fig. 9. Maximum strength vs lateral reinforcement.

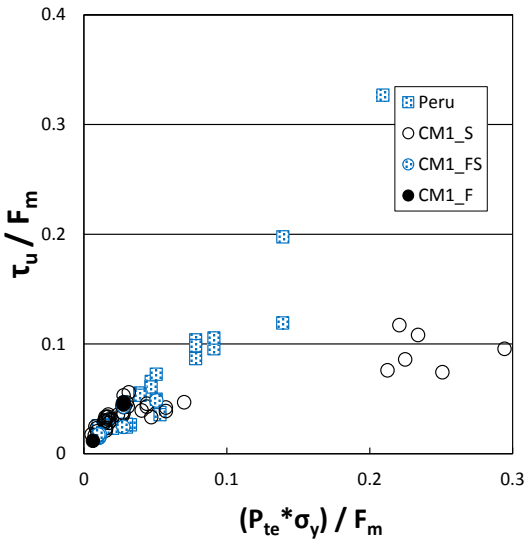

Fig. 8. Maximum strength vs flexural reinforcement.

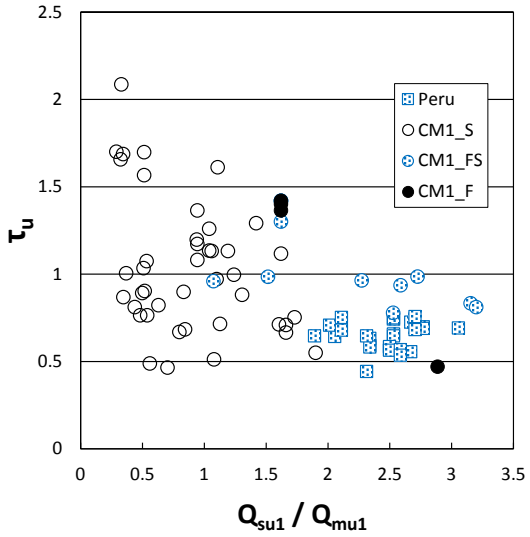

Fig. 10. Maximum strength vs margin of shear strength.

Figure 6 shows the relationship between observed maximum strength and the flexural strength as calculated by Eq. (3). It has been observed that Eq. (3) well estimates the maximum strengths of flexural (F) or flexural-shear failure (F-S) walls, the behavior of which have been affected by flexure, while it overestimates the maximum strength of shear failure (S) walls.

5. Analysis of the Maximum Strength

5.1. Factors Affecting the Maximum Strength

Figures 7 to **10** indicate the relationships between the observed maximum strength and factors affecting it, i.e., the axial stress ratio (σ_0/F_m), the amount of flexural reinforcement ($P_{te}\sigma_y$) normalized by the prism compressive strength (F_m), the amount of lateral reinforcement ($P_{we}\sigma_{wy}$) normalized by the prism compressive strength (F_m) and the margin of the shear strength, (Q_{su1}/Q_{mu1}: shear strength calculated using Eq. (1) / flexural strength calculated using Eq. (3)). The observed maximum strength normalized by the prism compressive strength τ_u/F_m increases with an increase in the axial stress ratio σ_0/F_m, the amount of flexural reinforcement $P_{te}\sigma_y/F_m$, and the amount of lateral reinforcement $P_{we}\sigma_{wy}/F_m$. It decreases with an increase in the margin of shear strength Q_{su1}/Q_{mu1}.

5.2. Regression Equation for the Maximum Strength

A multiple regression analysis was done for the observed maximum strength of all test walls (89 walls) considering the previously explained factors that affect it. The following empirical equations were then derived.

$$\tau_u = 1.57 + 3.23\frac{P_{we}\cdot\sigma_{wy}}{F_m} - 11.52\frac{\sigma_0}{F_m} - 0.31\frac{Q_{su1}}{Q_{mu1}} \quad (4)$$

$$\frac{\tau_u}{F_m} = 0.0038 + 0.26\frac{P_{te}\cdot\sigma_y}{F_m} + 0.14\frac{P_{we}\cdot\sigma_{wy}}{F_m} + 0.89\frac{\sigma_0}{F_m} \quad (5)$$

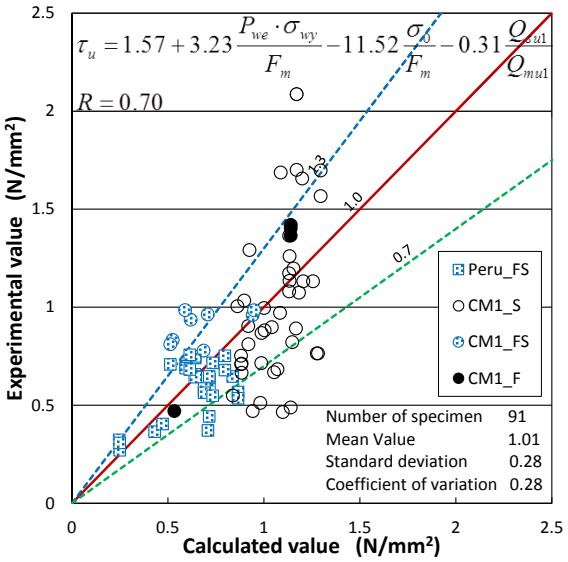

Fig. 11. Evaluation of the maximum strength with the proposed regression equation.

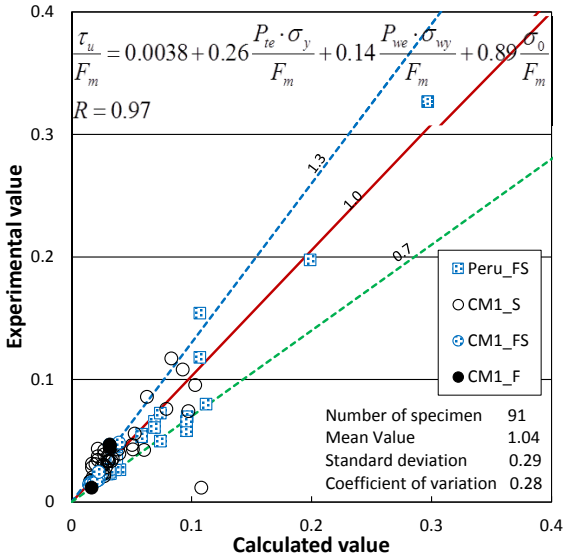

Fig. 12. Evaluation of the maximum strength using the proposed regression equation.

These equations globally predict the maximum strength of the walls despite the failure mode. Other empirical equations corresponding to each failure mode are derived, but they will be mentioned on another occasion. In Eq. (4), the maximum strength is expressed in terms of the average shear stress τ_u. The variables in the linear equation were the amount of lateral reinforcement ($P_{we}\sigma_{wy}$) normalized by the compressive strength of masonry prism (F_m), axial stress ratio (σ_0/F_m), and the margin of the shear strength (Q_{su1}/Q_{mu1}). The correlation coefficients of each factor to τ_u were 0.301, -0.509, and -0.490 for $P_{we}\sigma_{wy}/F_m$, σ_0/F_m, and Q_{su1}/Q_{mu1}, respectively. The strength calculated using Eq. (4) and that determined through tests are compared in **Fig. 11**. The coefficient of variation (standard deviation / mean value) is 28%, and 73% of the total number of walls are within 30% error. The correlation coefficient R is 0.70.

In Eq. (5), maximum strength is expressed in terms of the average shear stress τ_u normalized by the compressive strength of masonry prism F_m. The variables in the linear equation are the amount of lateral reinforcement ($P_{we}\sigma_{wy}$) and the amount of flexural reinforcement ($P_{te}\sigma_y$), respectively, normalized by the compressive strength of masonry prism F_m and the axial stress ratio (σ_0/F_m). The correlation coefficients to τ_u/F_m were 0.667, -0.589, and 0.411 for $P_{te}\sigma_y/F_m$, $P_{we}\sigma_{wy}/F_m$, and σ_0/F_m, respectively. The strength calculated using Eq. (5) and that determined through tests are compared in **Fig. 12**. The coefficient of variation is 28%, and 75% of the total number of walls are within 30% error. The correlation coefficient R is 0.97.

As shown in the figures above, these equations can predict the maximum strength of walls well regardless of their failure mode.

6. Analysis of Deformation at the Maximum Strength

6.1. Distribution of Deformation at the Maximum Strength $R_{\max}$

Figure 13 shows the distribution of the deformation at the maximum strength $R_{\max}$ in terms of the cumulative probability P_c($P_{c|R=Ri(\%)}$: P_c = Number of data$|_{R\leq Ri}$ / Total Number). The deformation $R_{\max}$ in the Japanese database (55 walls) ranges from 0.5 to 20×10^{-3} rad. while it ranges from 2.5 to 15×10^{-3} rad. in the Peruvian database (34 walls). However, the distribution curves are similar, both having an "s" shape.

Figure 14 shows the distribution of the deformation at the maximum strength $R_{\max}$ in terms of the probability density P_D (probability density P_D: $P_{D|R=R_m}$ (% per unit drift angle R_0) is the differential coefficient at $R = R_m$ on the $R - P_c$ curve). The deformation at the maximum probable density differs in the Japanese and Peruvian databases. The deformation at the most probable density is 4×10^{-3} rad. in the Japanese database while is larger, 7×10^{-3} rad., in the Peruvian database.

For reference, the distribution of the deformation at the maximum strength of reinforced concrete shear walls is shown in **Figs. 15** and **16**. These data come from a 1968 review by Tomii of 200 reinforced concrete shear walls [10]. According to **Fig. 15** which shows the cumulative probability of the deformation at maximum strength $R_{\max}$, the deformation ranges from 0.5 to 15×10^{-3} rad. The distribution curve is s-shaped, similar to the curves of confined brick walls seen in **Fig. 13**. The probability density of $R_{\max}$ is shown in **Fig. 16**. The deformation at the maximum probability density, at the peak of the distribution curve, is 4×10^{-3} rad. (drift angle of $1/250$). Since this figure was published, it has become well known that the deformation at the maximum strength of reinforced concrete shear wall is 4×10^{-3} rad. or $1/250$. In the standard for the seismic evaluation of reinforced concrete buildings, it is assumed that the shear failure member fails

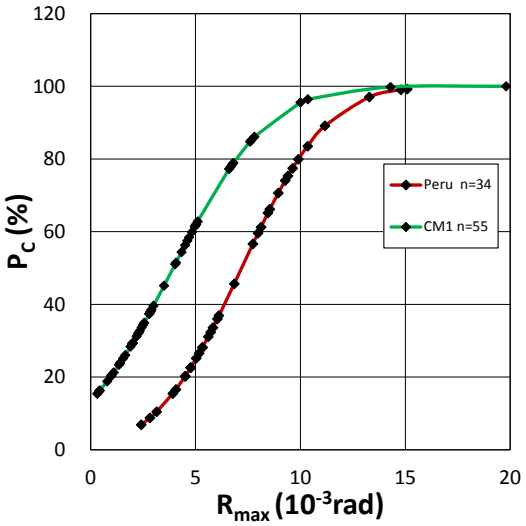

Fig. 13. Distribution of $R_{\max}$ of confined brick walls.

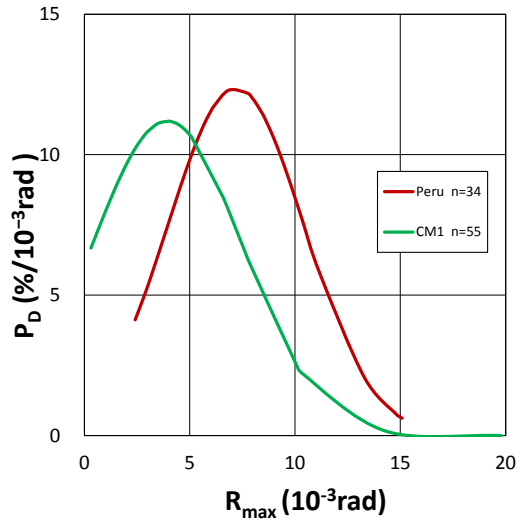

Fig. 14. Distribution of $R_{\max}$ of confined brick masonry walls.

in shear at the deformation 4×10^{-3} rad. or 1/250 [7]. This assumption is based on the distribution of $R_{\max}$ in **Fig. 16**.

6.2. Factors Affecting Deformation at the Maximum Strength R_{max}

The multiple regression analysis indicates that the shear span ratio (h/l) is the key factor in the deformation at maximum strength. It shows that deformation increases as the shear span ratio increases (**Fig. 17**). The correlation coefficient of $R_{\max}$ and h/l are 0.214. The effects of other factors are minor.

6.3. Regression Equations for Deformation at the Maximum Strength R_{max}

The following regression equation for the deformation at maximum strength $R_{\max}$ is derived in terms of the shear span ratio h/l.

$$R_{\max} = 0.41 + 5.7h/l \quad (\times 10^{-3} \text{ rad.}) \quad . \quad . \quad . \quad . \quad (6)$$

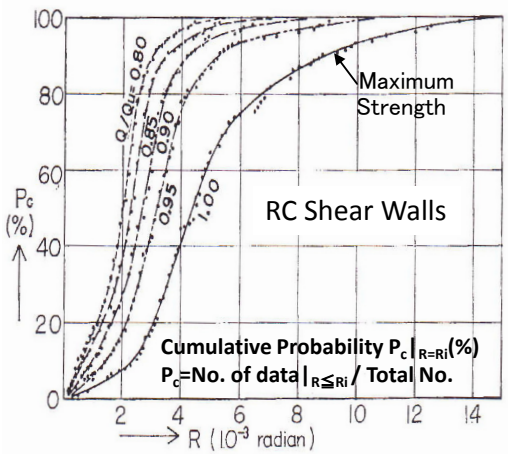

Fig. 15. Distribution of $R_{\max}$ of RC walls (after Tomii [10]).

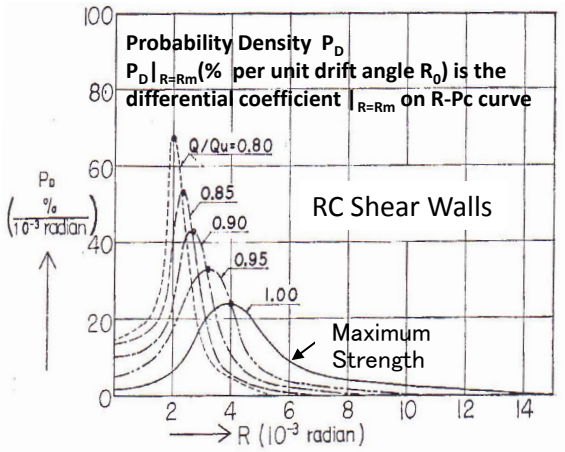

Fig. 16. Distribution of $R_{\max}$ of RC walls (after Tomii [10]).

The comparison between the calculated deformation by Eq. (6) and the observed deformation of $R_{\max}$ is shown in **Fig. 18**. The coefficient of variation to mean value is 77%, which is very large, and only 33% of the total number of walls are within 30% error. The correlation coefficient R is 0.43. The range of shear span ratios is from 0.52 to 2.09.

As indicated by these statistical values, the deformation at maximum strength can be evaluated using the empirical equation above, but there is a large amount of scatter.

7. Analysis of Deformation at the Ultimate State R_u

7.1. Distribution of Ultimate Deformation R_u

The distribution of the ultimate deformation R_u from both the Japanese and Peruvian databases is shown in terms of the cumulative probability P_c in **Fig. 19** and in terms of the probability density P_D in **Fig. 20**. The ultimate deformation R_u ranges from 1 to 19×10^{-3} rad. in the Japanese database and from 2 to 16×10^{-3} rad. in the Peruvian database. As seen in **Fig. 19**, the distribution forms "s" curves, as do those of $R_{\max}$ in **Fig. 13**.

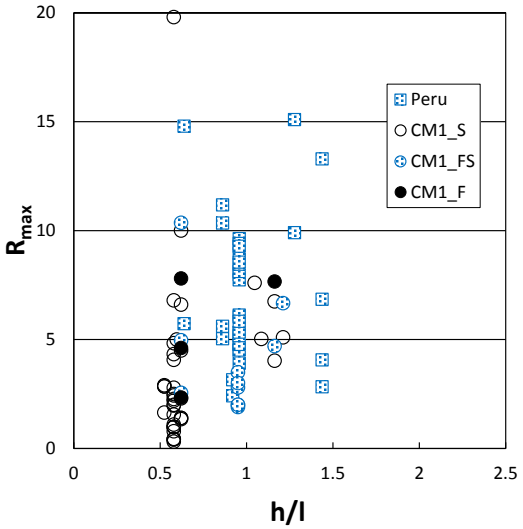

Fig. 17. Deformation at the maximum strength $R_{\max}$ vs shear span ratio h/l.

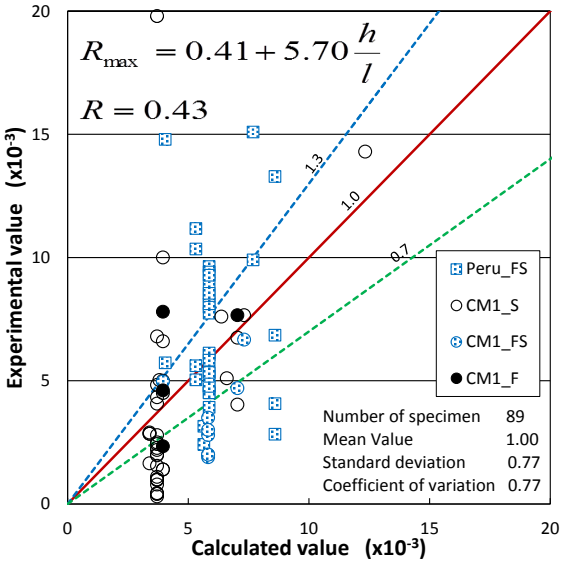

Fig. 18. Evaluation of the displacement at the maximum strength $R_{\max}$ using the proposed regression equation.

The deformation at the maximum probability density is 9×10^{-3} rad., which is 2.3 times the deformation at the maximum probability density of R_u in the Japanese database and 11×10^{-3} rad., which is 1.6 times the deformation at the maximum probability density of R_u in the Peruvian database.

7.2. Factors Affecting Ultimate Deformation R_u

The relationships between observed ultimate deformation R_u and the factors affecting it are shown in **Figs. 21** to **23**. The observed ultimate deformation is affected by the influencing factors as shown below.

It can be seen that the ultimate deformation R_u increases as the flexural reinforcement ($P_{te}\sigma_y/F_m$) increases for shear failure-type walls while it decreases for flexural or flexural-shear failure-type walls (**Fig. 21**). It can also

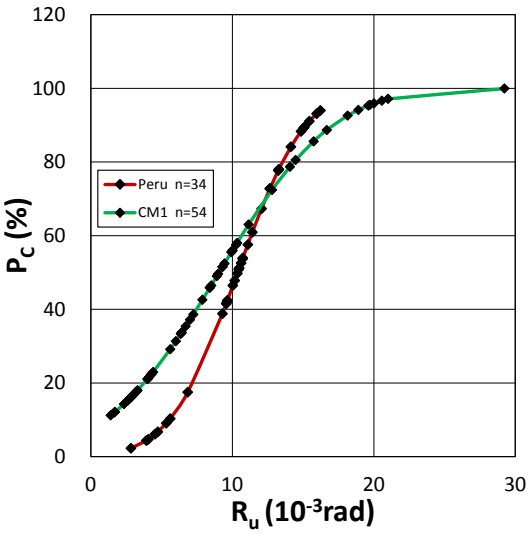

Fig. 19. Cumulative probability of P_c.

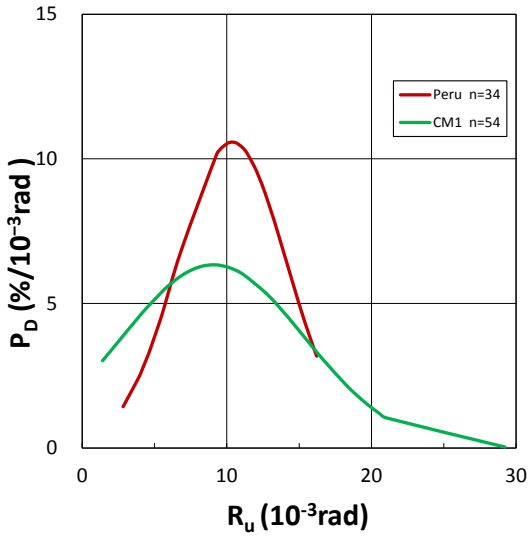

Fig. 20. Probability density of P_D.

be seen that R_u increases as the margin of shear strength Q_{su1}/Q_{mu1} increases (**Fig. 22**). The correlation coefficient of R_u and $P_{te}\sigma_y/F_m$ is 0.187, and that of R_u and Q_{su1}/Q_{mu1} is 0.138. The effect of axial stress ratio σ_0/F_m is not clear (**Fig. 23**).

7.3. Regression Equation for Ultimate Deformation R_u

The following linear regression equation for ultimate deformation R_u is derived in terms of the amount of flexural reinforcement $P_{te}\sigma_y/F_m$, axial stress ratio σ_0/F_m, and the margin of shear strength Q_{su1}/Q_{mu}.

$$R_u = 7.32 + 30.92\frac{P_{te}\sigma_y}{F_m} - 68.3\frac{\sigma_0}{F_m} + 1.47\frac{Q_{su1}}{Q_{mu1}} \quad (\times 10^{-3}\ \text{rad.}) \qquad (7)$$

Deformation values calculated using Eq. (6) are shown in **Fig. 24**. The coefficient of variation to mean value is 54%, smaller than that for $R_{\max}$, and 40% of the values for

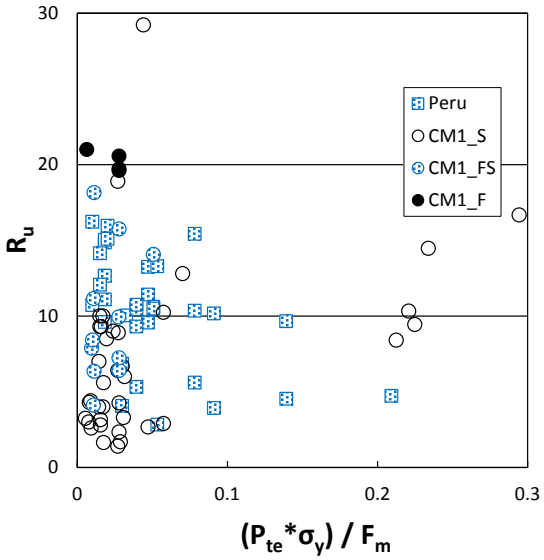

Fig. 21. Ultimate deformation R_u vs flexural reinforcement.

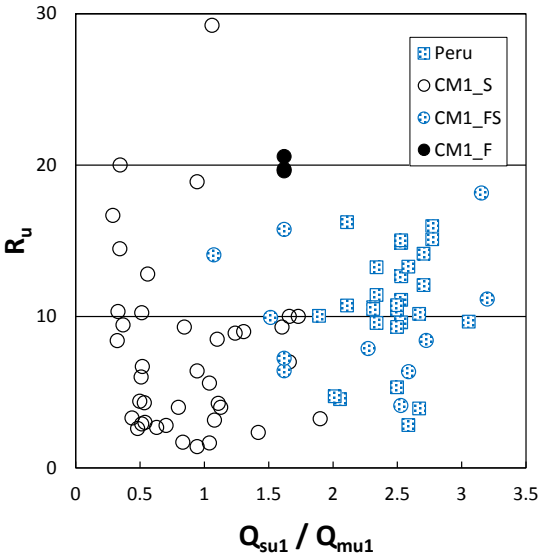

Fig. 22. Ultimate deformation R_u vs margin of shear strength.

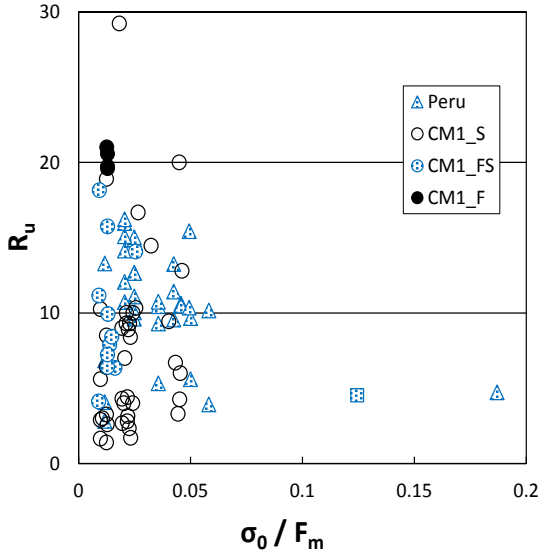

Fig. 23. Ultimate deformation R_u vs axial stress.

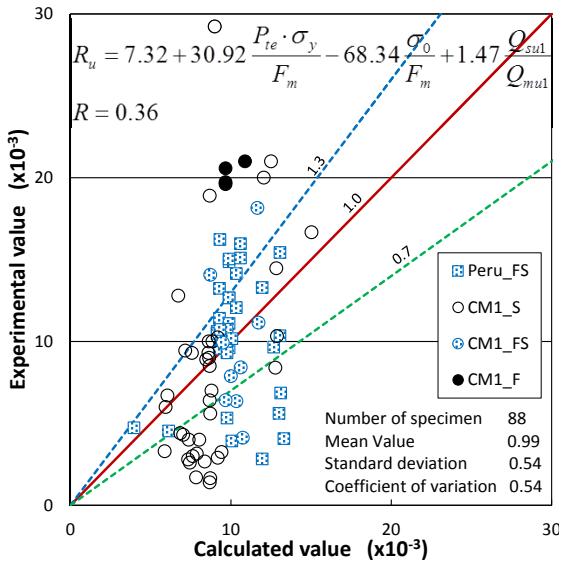

Fig. 24. Evaluation of the ultimate deformation R_u using the proposed regression equation.

the total number of walls are within 30% error. The range of $P_{te}\sigma_y/F_m$ is from 0.0055 to 0.29, that of σ_0/F_m is from 0.0 to 0.19, and that of Q_{su1}/Q_{mu1} is from 0.44 to 4.57.

8. Concluding Remarks

The results of tests on confined brick masonry walls in the Japanese database (55 walls) and Peruvian database (34 walls) were reviewed as one group of 89 walls in terms of failure mode maximum strength, deformation at maximum strength, and ultimate deformation. Results of the review can be summarized as follows.

(1) Applicability of existing equations used to estimate the maximum strength of confined brick masonry walls

The observed maximum strength of confined brick masonry walls was much smaller than the shear strength calculated using the existing equation for the ultimate shear strength of reinforced concrete shear walls.

The equation for the shear strength of hollow concrete block walls proposed by the Architectural Institute of Japan (AIJ) provided the average of the observed maximum strength of confined brick masonry walls, though the scatter of the evaluation was large.

The approximate equation for the ultimate flexural strength of reinforced concrete walls estimated the observed maximum strength of flexural or flexural-shear failure-type of confined brick masonry walls well, but it overestimated the maximum strength of the shear failure type of confined masonry walls.

(2) Deformation of confined brick masonry walls

The deformation at the maximum strength of confined brick masonry walls was equal to or larger than that of reinforced concrete shear walls (4×10^{-3} rad.). The ulti-

mate deformation was 1.6 to 2.3 times the deformation at maximum strength.

(3) Multiple regression analysis and empirical equations to estimate the maximum strength

The obtained empirical equation based on the multiple regression analysis of the maximum strength estimated the maximum strength of any type of failure mode of confined brick masonry walls with good accuracy and little error.

(4) Multiple regression analysis and empirical equations used to estimate deformations

The empirical equations obtained, which were based on the multiple regression analysis of the deformation at maximum strength and ultimate deformation, did estimate the deformations. However, as errors were large, the estimates were inaccurate.

Acknowledgements

This study was conducted as a part of the research project "Enhancement of Earthquake and Tsunami Disaster Mitigation Technology in Peru" supported by the Japan International Cooperation Agency (JICA) and the Japan Science and Technology Agency (JST).

References:

[1] H. Kato, T. Goto, and H. Mizuno, "Cyclic loading test of confined masonry wall elements for structural design development of apartment houses in the Third World," Proceedings of the Tenth World Conference on Earthquake Engineering (10WCEE), Madrid, Spain, 1992.

[2] K. Yoshimura and K. T. Kim, "Experimental Study for Higher Seismic Performance of Confined Brick Masonry Walls," Journal of Structural and Construction Engineering, Architectural Institute of Japan, No.571, pp. 169-176, Sept. 2003 (in Japanese).

[3] K. Yoshimura, K. Kikuchi, M. Kuroki, H. Nonaka, K. T. Kim, and A. Oshikata, "Experimental Study for Developing Higher Seismic Performance of Brick Masonry Walls," Proceedings of the 13th World Conference on Earthquake Engineering (13WCEE), Vancouver, Canada, August 2004.

[4] C. Zavala, P. Gibu, C. Homma, L. Chang, and G. Huaco, "Comportamiento Frente a Cargas Laterales de una Vivienda de Albañileria de Dos Pisos Mediante Ensayo en Linea," Proceedings of the XIV Congreso Nacional de Ingenieria Civil – Iquitos, Peru, 2003 (in Spanish).

[5] C. Zavala, C. Homma, P. Gibu, and G. Huaco, "Sesimic Behavior of Two Stories Masonry Building," Proceedings of Japan-Peru Workshop on Earthquake Disaster Mitigation, Lima, 2005.

[6] R. Salinas, F. Lázares, "La Alnañilería Tubular y su Uso en Viviendas en Zona Sísimicas," Proc. of the Conferncia Internacianal en Ingenieria Sísmica, Agost, 2007 (in Spanish).

[7] Japan Building Disaster Prevention Association, "Standard for Seismic Evaluation of Existing Reinforced Concrete Buildings, 2001 and Guidelines for Seismic Retrofit of Existing Reinforced Concrete Buildings, 2001," English Version, 1st, January, 2005.

[8] Architecrural Institute of Japan, "Ultimate Strength and Deformation Capacity of Buildings in Seismic Design (1990)," October, 1990 (in Japanese).

[9] A. Matsumura, "Shear Strength of Reinforced Masonry Walls, Proceedings of the 9th World Conference on Earthquake Engineering, pp. VI-121-126, Tokyo, Kyoto, 1988.

[10] M. Tomii and M. Takeuchi, "The Relations between the Deformed Angle and the Shearing Force Ratio (0.80 – 1.00) with Regard to 200 Shear Walls," Transaction of Architectural Institute of Japan, No.153, November 1968.

Name:
Shunsuke Sugano

Affiliation:
Visiting Research Fellow/Lecturer, Building Research Institute

Address:
1-Tatehara, Tsukuba, Ibaraki, Japan

Brief Career:
1971- Joined Takenaka Corporation, Technical Research Laboratory
2000- Professor, Hiroshima University
2009- Visiting Research Fellow/Lecturer, Building Research Institute

Selected Publications:
• S. Sugano (Ed.), "Seismic Rehabilitation of Reinforced Concrete Structures," International Publication Series 2 (IPS-2), American Concrete Institute, 2007.
• S. Sugano, "Lessons on Seismic Rehabilitation of Reinforced Concrete Buildings Learned from Recent Earthquakes," Proceedings of the Symposium Honoring Jim Jirsa, American Concrete Institute, 2014.

Academic Societies & Scientific Organizations:
• Architectural Institute of Japan (AIJ)
• Japan Concrete Institute (JCI)
• American Concrete Institute (ACI)
• Earthquake Engineering Research Institute (EERI)
• Japan Association for Earthquake Engineering (JAEE)